Ab initio calculation of spin-dependent electron-phonon coupling in iron and cobalt

Matthieu J. Verstraete[1,2]

[1] Unité Nanomat, Université de Liège, allée du 6 août, 17, B-4000 Liège, Belgium and
[2] European Theoretical Spectroscopy Facility http://www.etsf.eu

PACS numbers: 72.25.-b, 71.15.Mb, 63.20.kd

Abstract. The spin-dependent coupling between electrons and phonons in ferromagnetic Fe and Co is calculated from first principles in a collinear-spin formalism. The added spin polarization is fundamental for the correct representation of the phonons, but also to obtain good transport properties, and permits the decomposition (e.g. of the resistivity) into the contributions of majority and minority spin. In Fe the minority spin coupling is only about 50% more important, but in Co the coupling between phonons and minority spin electrons is an order of magnitude larger than majority, and both are strongly anisotropic.

1. Introduction

The coupling of electron spin and vibrations in solids has garnered renewed interest in the past decade, after a lull since the 60s and 70s. Specific momentum comes from the fields of spintronics[1], where phonon processes limit the lifetime of spins in matter, caloritronics[2] where heat and spin currents are coupled, and superconductivity, where cuprate[3] and pnictide[4] systems present complex interactions between spin, phonon, and superconducting degrees of freedom. For the latter there is growing consensus that magnetic fluctuations and antiferromagnetic order play a central role in explaining the Cooper pairing and the high transition temperatures observed. More widely, the temperature dependence of magnetic processes is central to important physical phenomena such as the geodynamics of the Earth's core[5]. The prediction of spin-phonon processes in condensed matter systems is of wide interest, but the success enjoyed by first-principles calculations of ground state properties has been slow to carry over to the full temperature dependence of predicted properties. This is due to the inherent complexity of the coupling, the large number of different mechanisms in play (in particular anharmonic vibrational effects), and the range of pertinent length and time scales.

In the following the electronic and vibrational properties of bulk Fe and Co are calculated using spin-polarized density functional theory (DFT[6, 7]) and density functional perturbation theory (DFPT[8, 9, 10]). Fe and Co are paradigmatic ferromagnets, and technologically very important, in particular for the exotic applications in superconductivity and spintronics mentioned above. The electron-phonon coupling (EPC) is calculated using a (collinear) spin-dependent formulation. Though never strictly correct as there will always be a small contribution from spin-orbit coupling in real systems, the physical picture of separate spin channels is very appealing and very accurate for strongly polarized ferromagnets and many anti-ferromagnets as well (as long as spin canting is negligible). The present developments should be used in this context and to provide a reference picture for more complex cases where weak spin-mixing occurs, which can be treated perturbatively. The consequences on the electrical and thermal transport properties are analyzed and provide very different pictures for Fe (isotropic and strong coupling) and Co (very anisotropic coupling and weaker resistivities). Results agree generally very well with experiment where available. To our knowledge only two calculations of the spin-polarized EPC within DFT have been published, by Boeri et al.[11], for $BaFe_2As_2$, and by Sha and Cohen[12] for hcp and bcc Fe under pressure (though the latter did not explain their treatment of spin, we presume it is complete). A very recent paper by Pozzo et al.[5] calculates conductivities in Fe under pressure via the Green-Kubo formulas, but without direct access to the EPC. Essert and Schneider[13] have calculated magnetization dynamics in Ni and Fe with mainly ab initio ingredients, but using the atomic sphere approximation for the EPC. Jarlborg[14] has calculated the EPC in Fe and Co under pressure in their non-magnetic state but including magnetic fluctuations. A rather complete account of the

thermodynamics of ferromagnetic Fe has been given by Körmann et al.[15].

In the following Hartree atomic units have been used, except where explicitly stated, with energy in Hartree (Ha = 27.211 electron volts), distances in bohr radii ($a_0 = 0.529$ Å), and with units of electron charge and mass, with Planck's constant equal to 1 ($e = \hbar = m_e = 1$).

2. Spin-dependent generalizations

The standard approach for calculating electron-phonon coupling parameters from first principles is based on seminal papers by PB Allen[16, 17], and the first systematic implementation in DFT by Savrasov and Savrasov[18]. The deformation potential and its matrix elements are calculated self-consistently along with the DFT solution for the dynamical matrix. The matrix elements can then be summed over the Fermi surface, and various quantities extracted, in particular phonon line widths, self-energy (Eliashberg) spectral functions, and electrical and thermal transport coefficients. The Boltzmann transport equations are solved in a simplified ansatz, and the lowest order variational approximation (LOVA) is taken to give closed forms for the transport coefficients. In the following we briefly present the spin-dependent generalization of these equations, and restrict ourselves to the collinear case. If spin-orbit coupling is present the electron bands are of mixed spin character and the EPC can flip spins, in a variety of mechanisms (detailed for example in Ref [1]).

The equations written down by Eliashberg and implemented by Allen[17] then Savrasov[18] are naturally expressed in terms of the density of states per spin, and the matrix elements of the deformation potential using individual electron orbitals, as they come from a Cooper-pair context with anomalous Green's functions. If spin-orbit interaction is excluded, there is no (normal state) coupling between space (or angular momentum) and spin which would allow the EPC distortion to mix different-spin orbitals. The matrix elements and density of states stay spin-diagonal and give the following expressions (some are mentioned in passing in Ref. [11]):

$$g^{\mathbf{q}\nu}_{n'\mathbf{k}+\mathbf{q}\sigma' \; n\mathbf{k}\sigma} = \delta_{\sigma\sigma'} \langle \psi_{n' \, \mathbf{k}+\mathbf{q} \, \sigma'} | \delta V^{\mathbf{q}\nu} | \psi_{n \, \mathbf{k} \, \sigma} \rangle \tag{1}$$

where ν is an phonon mode, $\mathbf{q}$ a phonon wave vector, n, n' electron band indices, $\mathbf{k}, \mathbf{k}'$ electron wave vectors, δV is the self-consistent potential change due to an infinitesimal phonon displacement, and σ, σ' the spin component of the Pauli spinors. If the spin-orbit coupling is included, each orbital is a true spinor, and there is an arbitrary gauge coming from the choice of reference frame for L and S. The consistent quantity to calculate is the full scalar product

$$g^{\mathbf{q}\nu}_{n'\mathbf{k}+\mathbf{q} \; n\mathbf{k}} = \sum_{\sigma\sigma'} \langle \psi_{n' \, \mathbf{k}+\mathbf{q} \, \sigma'} | \delta V^{\mathbf{q}\nu}_{\sigma'\sigma} | \psi_{n \, \mathbf{k} \, \sigma} \rangle \tag{2}$$

which no longer possesses gauge variability due to the spin, but neither does it give access to separate spin flip probabilities: the transition is from one general spinorial state n to another n'. To recover the change in spin between kn and $k'n'$ one needs

the Pauli matrix elements $\sum_{\sigma\sigma'}\langle\psi_{n\mathbf{k}\sigma}|\bar{\sigma}^{\alpha}_{\sigma\sigma'}|\psi_{n'\mathbf{k}'\sigma'}\rangle$. The rest of this article considers the collinear spin case only: Fe and Co present fairly weak spin orbit coupling. Their non-collinear spin waves have been studied extensively[19, 20] but present additional complications beyond the scope of the present analysis.

From the matrix elements one proceeds to calculate the phonon linewidths, which can now be separated into a width due to coupling with spin up electrons and another due to coupling with spin down electrons (the inverse lifetimes are additive):

$$\gamma^{\sigma}_{\mathbf{q}\nu} = 2\pi\omega_{\mathbf{q}\nu}\sum_{\mathbf{k}nn'}|g^{\mathbf{q}\nu}_{n'\mathbf{k}+\mathbf{q}\sigma\ n\mathbf{k}\sigma}|^2\delta(\epsilon_{\mathbf{k}n\sigma})\delta(\epsilon_{\mathbf{k}+\mathbf{q}n'\sigma}) \tag{3}$$

where the Fermi energy ϵ_F is set to 0 for convenience. ϵ_F is presumed common to both spin channels, though this is not strictly necessary. The corresponding spectral functions for the EPC self-energy are

$$\alpha^2F^{\sigma}(\omega) = \frac{1}{2\pi N^{\sigma}(\epsilon_F)}\sum_{\mathbf{q}\nu}\frac{\gamma^{\sigma}_{\mathbf{q}\nu}}{\omega_{\mathbf{q}\nu}}\delta(\omega-\omega_{\mathbf{q}\nu}) \tag{4}$$

The same straightforward spin generalizations are valid for the transport Eliashberg functions:

$$\begin{aligned}\alpha^2_{\mathrm{out(in)}}F^{\sigma}_{\alpha\beta}(\omega) = \frac{1}{2\pi N^{\sigma}(\epsilon_F)}\sum_{\nu}\sum_{\mathbf{k}\mathbf{k}'nn'}|g^{\mathbf{k}'-\mathbf{k}\nu}_{n'\mathbf{k}'\sigma\ n\mathbf{k}\sigma}|^2 \\ \times\frac{v_{\alpha}(n\mathbf{k}\sigma)}{<v_{\alpha}(\sigma)>}\frac{v_{\beta}(n^{(\prime)}\mathbf{k}^{(\prime)}\sigma)}{<v_{\beta}(\sigma)>} \\ \times\delta(\epsilon_{\mathbf{k}n\sigma})\delta(\epsilon_{\mathbf{k}'n'\sigma})\delta(\omega-\omega_{\mathbf{k}'-\mathbf{k}\nu})\end{aligned} \tag{5}$$

where α,β are cartesian directions, and the difference between the out and in transport spectral functions is the choice of the k-point at which the second velocity is evaluated at ($\mathbf{k}$ or $\mathbf{k}'$). The Fermi speed $v_{\alpha}(n\mathbf{k}\sigma)$ is now also spin dependent, and the normalization factors are given by:

$$<v_{\alpha}(\sigma)>^2 = \frac{1}{N^{\sigma}(\epsilon_F)}\sum_{\mathbf{k}n}|v_{\alpha}(n\mathbf{k}\sigma)|^2\delta(\epsilon_{\mathbf{k}n\sigma}) \tag{6}$$

The transport spectral function is $\alpha^2_{\mathrm{tr}}F^{\sigma}_{\alpha\beta} = \alpha^2_{\mathrm{out}}F^{\sigma}_{\alpha\beta} - \alpha^2_{\mathrm{in}}F^{\sigma}_{\alpha\beta}$ and gives the electrical and thermal resistivities:

$$\rho^{\sigma}_{\alpha\beta}(T) = \frac{2\pi\Omega k_BT}{N^{\sigma}(\epsilon_F)}\int_0^{\infty}\frac{d\omega}{\omega}\frac{x^2}{\sinh^2 x}\alpha^2_{\mathrm{tr}}F^{\sigma}_{\alpha\beta}(\omega) \tag{7}$$

and

$$\begin{aligned}w^{\sigma}_{\alpha\beta}(T) = \frac{6\Omega_{cell}}{\pi k_BN^{\sigma}(\epsilon_F)}\int\frac{d\omega}{\omega}\frac{x^2}{\sinh^2 x} \\ \times\quad\left[\alpha^2_{\mathrm{tr}}F^{\sigma}_{\alpha\beta}(\omega)+\frac{4x^2}{\pi^2}\alpha^2_{\mathrm{out}}F^{\sigma}_{\alpha\beta}(\omega)+\frac{2x^2}{\pi^2}\alpha^2_{\mathrm{in}}F^{\sigma}_{\alpha\beta}(\omega)\right]\end{aligned} \tag{8}$$

with $x = \omega/2k_BT$ (the notations follow Ref. [18], which is missing a factor of 2 in equation 21 for the resistivity). Care must be taken in normalizing quantities per spin - the phonon observables (λ, γ) should be summed over spin polarizations, whereas the electronic quantities (ρ, w, N) are spin-specific.

The resulting spin-decomposed resistivity gives an appealing physical picture of the limitation of the current in each of the spin channels. However, as will be seen below in comparison to experiment, the two channels are not purely parallel resistors in reality. Spin flip mechanisms (in particular spin-orbit) force them to interfere, and make the effective resistivity a weighted average of $\rho^{\uparrow}$ and $\rho^{\downarrow}$. This is further augmented by the impurity, defect, magnon, and other mechanisms for electrical resistivity which we do not calculate here. The LOVA approximation has a limited range of applicability, explained clearly in Ref. [18], for approximately $\Theta_{tr}/5 < T < \Theta_{tr}$ where we define the average frequency

$$\Theta_{tr} = \sqrt{\int \alpha^2 F_{tr}(\omega)\omega^2 d\omega / \int \alpha^2 F_{tr}(\omega) d\omega} \tag{9}$$

Beyond Θ_{tr} anharmonic and higher order EPC effects can and often do appear, leading to non-linear $\rho(T)$ curves, and shifts in phonon frequencies and thermal expansion. In many cases with weak anharmonicity and thermal expansion, however, the range of linearity and validity of the LOVA can be much wider than Θ_{tr}, as is seen in Ref. [18].

3. Calculation details

The Kohn-Sham DFT equations are solved using the implementation in the ABINIT[21] package. Norm-conserving pseudopotentials are employed for the electron-ion interaction, and generated using the OPIUM[22, 23] package. They incorporate scalar relativistic corrections, non-linear core corrections[24], and the PBE[25] generalized gradient approximation (GGA) exchange-correlation functional. A plane-wave kinetic energy cutoff of 50 Ha is necessary to ensure convergence of phonon frequencies well below 0.1%. No Hubbard correction (LDA+U[26]) is used; the magnetism and lattice constants are well enough reproduced for our purposes here, and to improve on this precision all-electron methods are usually necessary. The lattice is converged to stresses less than 10^{-6} Ha/bohr^3. A gaussian smearing function of width 1mHa is used to accelerate the convergence with respect to the k-point grid.

For hcp Co a 9 valence electron pseudopotential is used, and gives lattice constants of a=4.79 and c=7.75 bohr, versus 4.73 and 7.69 experimentally[28]. Zone-centered grids of 16^3 k-points for electrons and 8^3 q-points for phonons are necessary to capture the delicate Fermi Surface effects in the phonons and EPC. The magnetic moment per atom is 1.67 μ_B (Bohr magneton), similar to other results (e.g. 1.61 in PBE, 1.72 experimentally, and 1.83 with GGA+U, all from Ref. [29]). The resulting density of states (DOS) at the Fermi level are 4.957 (22.459) states/Ha/atom for spin up (resp. down), slightly higher than 4.58 (20.72) found in Ref. [30].

The Iron nucleus is replaced by an 8 valence electron pseudopotential, and gives a cubic BCC lattice parameter of 5.328 bohr (compared to an experimental value of 5.41 bohr[31]). Reciprocal space grids of 12^3 points are used both for the electronic and phononic degrees of freedom (a 24^3 grid for electrons is used punctually to verify convergence of phonons and the EPC quantities at Γ). The magnetic moment per

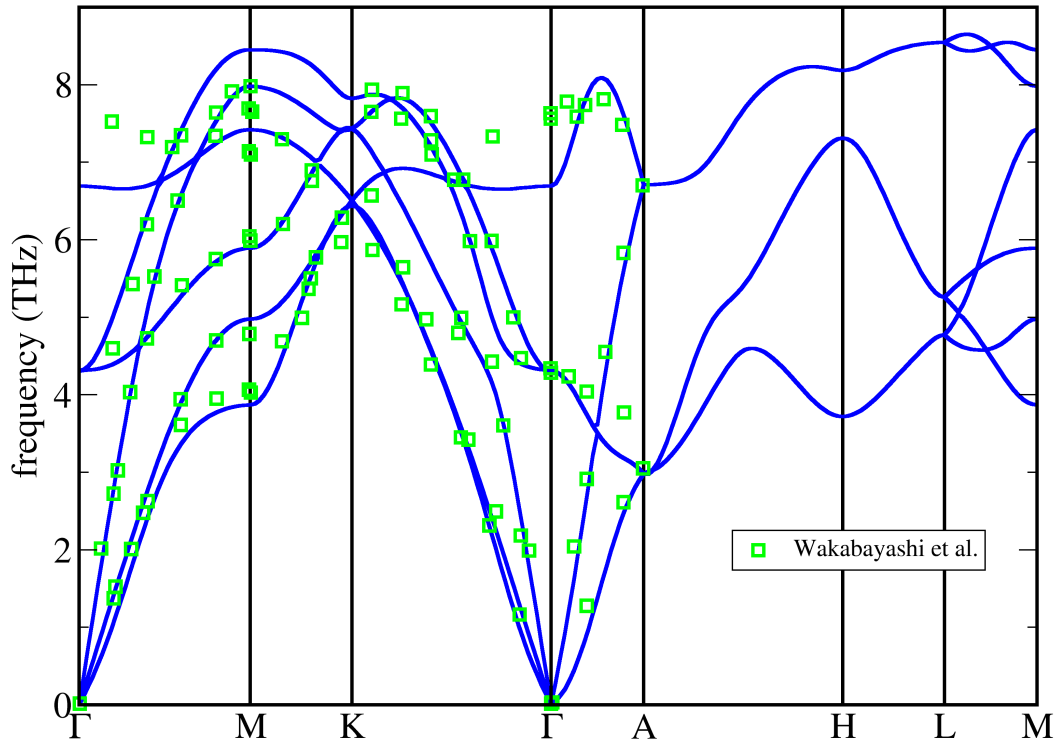

Figure 1. Phonon band structure for spin polarized Co, compared to experimental data from Ref [27]. Overall agreement is quite good, with the exception of the last phonon branch at Γ.

atom is 2.335 μ_B, reasonably close to the experimental and GGA-PW values of around 2.2[31, 32]. The DOS at the Fermi level is 14.12 (8.49) states/Ha for spin up (resp. down), which is in reasonable agreement with LSDA calculations 18.80 (7.75) from Ref. [33], given the very abrupt nature of the d-band DOS (the integrated value of μ is more robust). The experimental value of 54.74 states/Ha[34] for the total DOS is much higher, and is claimed to come from phonon- and magnon- renormalized band masses (the mass renormalization from the DOS values is $\lambda_{eff} \sim 1.4$ comparing our calculated DOS to experiment).

The underestimation of the volume in Fe is strange for the GGA functional, but agrees with previous theoretical work, and is probably related to the approximate treatment of the magnetism in "normal" DFT (i.e. without LDA+U).

A real space cutoff for interatomic force constants beyond 20 bohr distance is used to remove Fourier transform aliasing errors near the Γ point. The error introduced on frequencies at q-points away from Γ is at most 3% (6%) and on mean square average less than 1% (2%) for Fe (resp. Co). A slight artificial bowing of the acoustic branches is also introduced, but this does not affect integrated quantities.

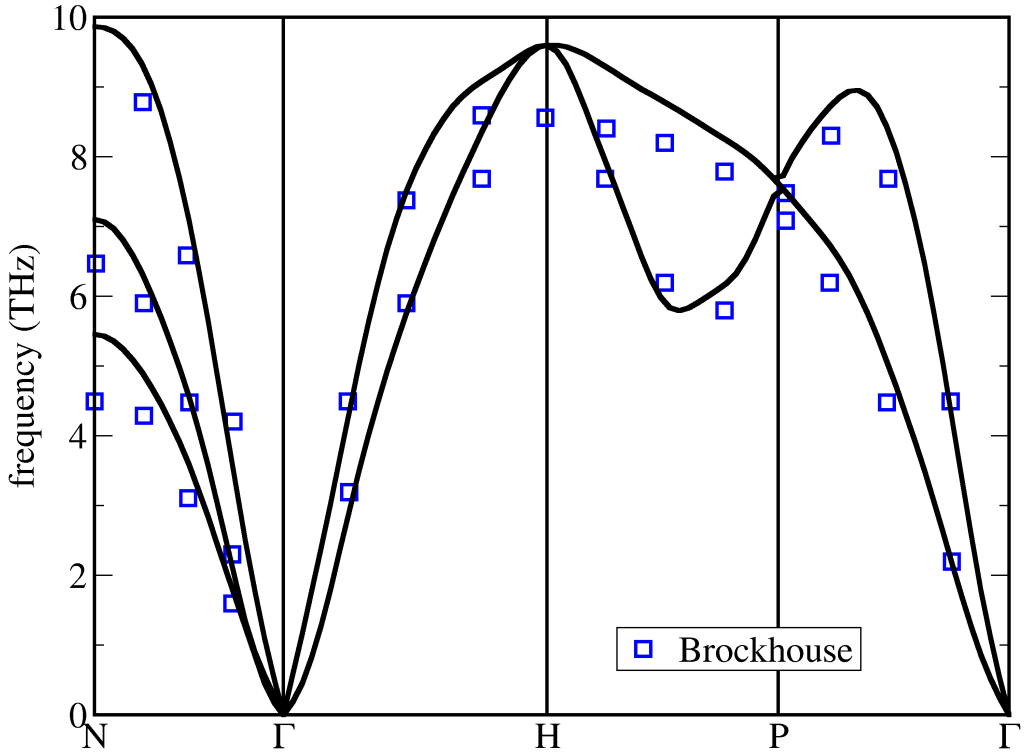

Figure 2. Phonon band structure for spin polarized Fe, compared to experimental data from Refs [35]. Overall agreement is quite good, with a small hardening of the calculated phonons due to the underestimation of the equilibrium volume.

4. Phonons, EPC and transport

As shown by many other authors (e.g. Ref. [36]), the correct inclusion of ferromagnetic electronic states is essential for the calculation of the phonon band structures. In particular the BCC phonon band structure for Fe presents strong instabilities through the whole Brillouin Zone if calculated in a non-spin-polarized formalism. The phonon band structures for Cobalt and Iron are shown in Fig. 1 and 2. In Fe the phonons are slightly harder than experimental frequencies, due to the smaller equilibrium volume. In Co the agreement is better except for the last optical branch, which is both over and underestimated in different regions of the Brillouin Zone.

Experiments and calculations on cobalt are much less common than iron. Wakabayashi et al.[27] published neutron experiments in 1982, and Madok[37] calculated thermodynamical properties without showing full phonon band structures. Our calculation of the full band structure is in good agreement with the experimental data, except for the highest branch at Γ (the optical mode along z). This is the mode with strongest electron-phonon coupling, as seen in Fig. 3, where the error bars show the calculated phonon line widths $\gamma^{\sigma}_{\mathbf{q}\nu}$. Correcting the last mode at Γ will probably require

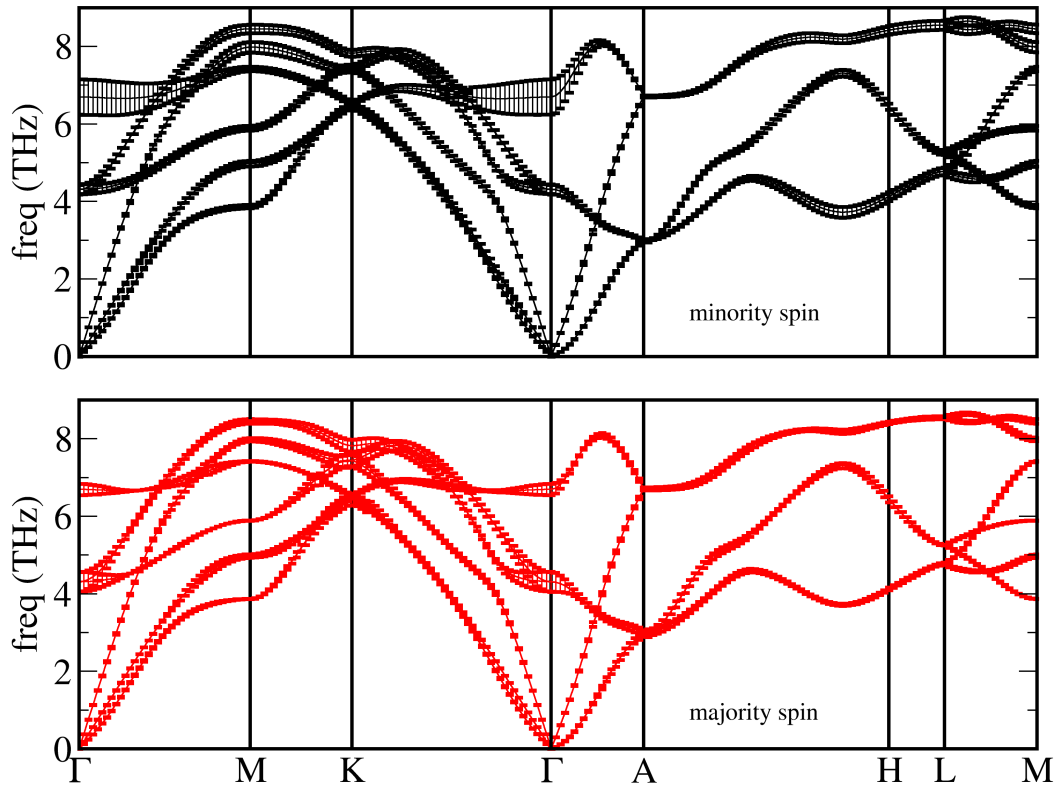

Figure 3. Phonon band structure for HCP Co with band widths given by the phonon broadening due to EPC. The lifetimes due to majority spin electrons have been multiplied by 20 to make them visible.

going beyond the GGA for exchange and correlation. The majority and minority spin electrons couple very differently as a function of $\mathbf{q}$, and have a more than 1 order of magnitude difference in amplitude.

For iron a large literature of calculations exists for phonons, and our Fe data agrees well with published calculations and with the experiments by Brockhouse[35] at ambient conditions. In Fig. 4 the bands are shown with their calculated linewidths showing the respective coupling to majority and minority spin electrons. The latter is larger by a factor of 2-5 depending on $\mathbf{q}$.

The electron phonon coupling is usually summarized by the dimensionless coupling constant $\lambda = \int \alpha^2 F/\omega d\omega$, and the corresponding inverse moments of the transport spectral functions $\lambda_{tr} = \int \alpha^2 F_{tr}/\omega d\omega$. In the spin polarized case the two spectral functions give two coupling constants $\lambda^{\uparrow}$ and $\lambda^{\downarrow}$. Our calculated values are shown in table 1 for λ, and table 2 for λ_{tr}. The values of λ are of moderate strength for Fe and quite strong for Co. In both cases the majority spin coupling is significantly weaker - this corresponds to the type of bands at E_F in each case: end of the d band for Fe and the s band for Co, whereas the minority spin band is in the middle of the d band. The correlation is not directly with the amplitude of the DOS for each spin, but a combined

effect with the nature of the bands - localized d states feel a stronger effect from the displacement of a phonon mode. In iron the experimental $N(\epsilon_F)$ enhancement is only partly accounted for by EPC: 0.243 out of an enhancement of 1.4.

	$\lambda^{\uparrow}$	$\lambda^{\downarrow}$	λ^{tot}
Co	0.182	1.134	1.316
Fe	0.068	0.175	0.243

Table 1. Electron phonon coupling constants for spin polarized Fe and Co.

	$\lambda^{\uparrow}_{tr,xx}$	$\lambda^{\uparrow}_{tr,zz}$	$\lambda^{\downarrow}_{tr,xx}$	$\lambda^{\downarrow}_{tr,zz}$	$\frac{1}{3}Tr[\lambda^{\mathrm{tot}}_{tr}]$
Co	0.002	0.001	0.008	0.024	0.015
Fe	0.102	-	0.199	-	0.300

Table 2. Electron phonon transport coupling constants for spin polarized Fe and Co.

The value of $\lambda^{\mathrm{tot}}_{tr} = \lambda^{\uparrow}_{tr} + \lambda^{\downarrow}_{tr}$ for Fe agrees very well with the result of Sha and Cohen (0.31). For Co the drastic reduction of λ_{tr} with respect to λ is due to the Fermi velocity factors in $\alpha^2 F_{tr}$. In cobalt the coupling constants and spectral functions are anisotropic, and the directional dependency in Eq. 5 yields two inequivalent directions for Co ($xx = yy \neq zz$). The tensors should stay diagonal for both systems: the calculated cross terms give an estimate of the numerical accuracy of the calculation, and are about 100 times smaller than the diagonal terms (no explicit symmetrization of the σ matrix is imposed, as a check).

The principal experimental quantity which bears witness to the electron-phonon coupling is the resistivity, shown for Co and Fe in figures 5 and 6, as a function of temperature. The cobalt data at high temperature should be compared critically: the crystalline phase is different (fcc) above 660 K up to the melting point at 1768 K. The anisotropy in resistivity predicted here might be visible for individual grains or isolated nanocrystals. The spin polarization of ρ is very strong: $\rho^{\uparrow}$ is close to zero. Eliminating impurities would allow a larger part of the current to flow in the spin up channel, but spin orbit coupling will always prevent the creation of a completely polarized current. The experimental spin diffusion lengths in Co are quite large for a ferromagnetic metal, between 40 nm (at 4.2 and 300 K) and 60 nm (at 77 K)[38]. This is probably linked to weak spin-orbit coupling and the strong difference in EPC between the two spins which we calculate here: the majority spins diffuse very little, and the minority spin electrons diffuse more strongly, but without flipping their spin as spin-orbit coupling is weak. The curves that can be seen at the bottom of figure 5 are majority spin diagonal terms (σ_{xx}, σ_{yy}, σ_{zz}) and minority spin off-diagonal terms (σ_{xy} etc...). The former are small for the physical reasons explained, while the latter should be 0 by symmetry, and show the numerical error - as mentioned above they are at most 2% of the diagonal terms ($2{\cdot}10^{-9}\Omega m$ at 1000 K), even in the very low resistivity Co case. This is also true

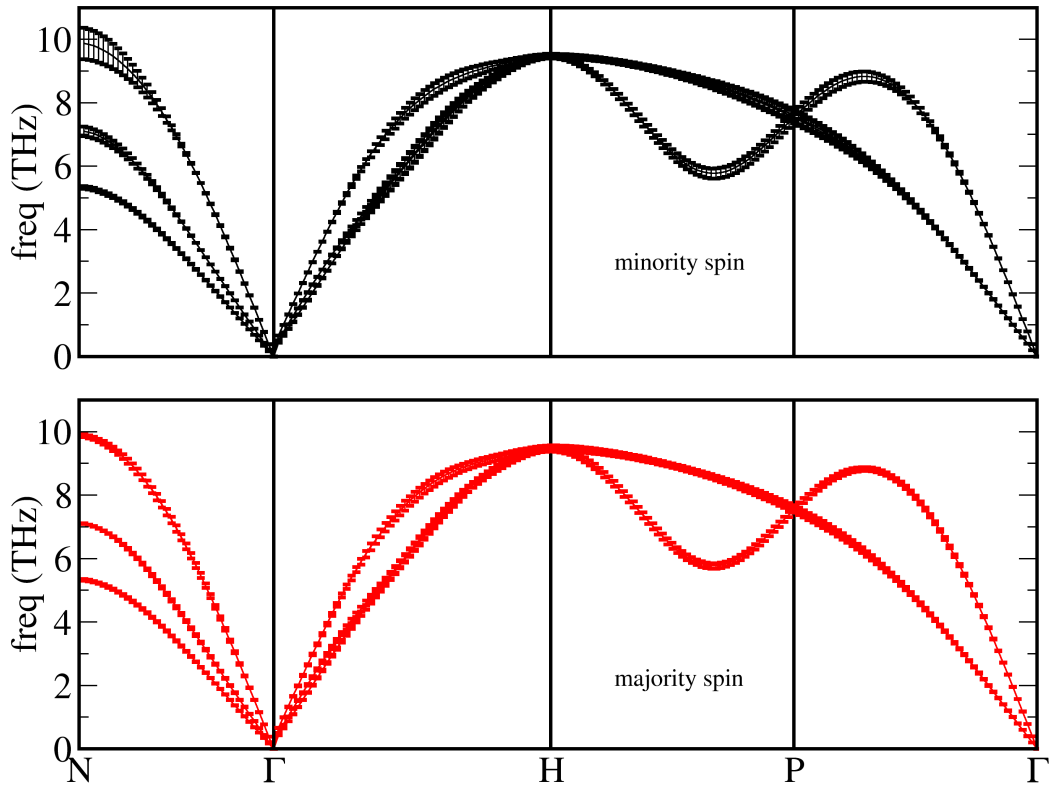

Figure 4. Phonon band structure for BCC Fe with band widths given by the phonon broadening due to EPC, for majority and minority spins. All linewidths have been multiplied by a factor of 5 for visibility.

for the majority spin channel, where the off-diagonal terms are even smaller in absolute value ($2{\cdot}10^{-10}\Omega m$ at 1000 K).

The picture of transport in Fe is very different from Co: both spin channels have larger resistivities. The minority spin channel is again more resistive (larger EPC). The experimental data lie between the two curves for $\rho^{\uparrow}$ and $\rho^{\downarrow}$. The experiment corresponds to a mixed situation where the spin channels interfere instead of conducting in parallel. The experimental diffusion length in Fe is only 8.5 nm at 4.2 K[38], which correlates with the higher resistivity.

The thermal conductivity contribution from EPC can also be calculated from the transport spectral functions. This describes the limitation of heat transport by electrons (due to scattering off phonons) and of heat transport by phonons (due to scattering off electrons). No anharmonic effects are included: their main consequences are 1) to limit the phonon lifetime and conductivity, and to 2) change the phonon distribution function, leading to a modified electron heat transport as well (this is a higher order effect). Figures 7 and 8 show the thermal conductivity as a function of temperature for Co and Fe (resp.), along with available experimental data. As for the electrical resistivity the agreement for Fe is quite good, though at high temperature there is clearly

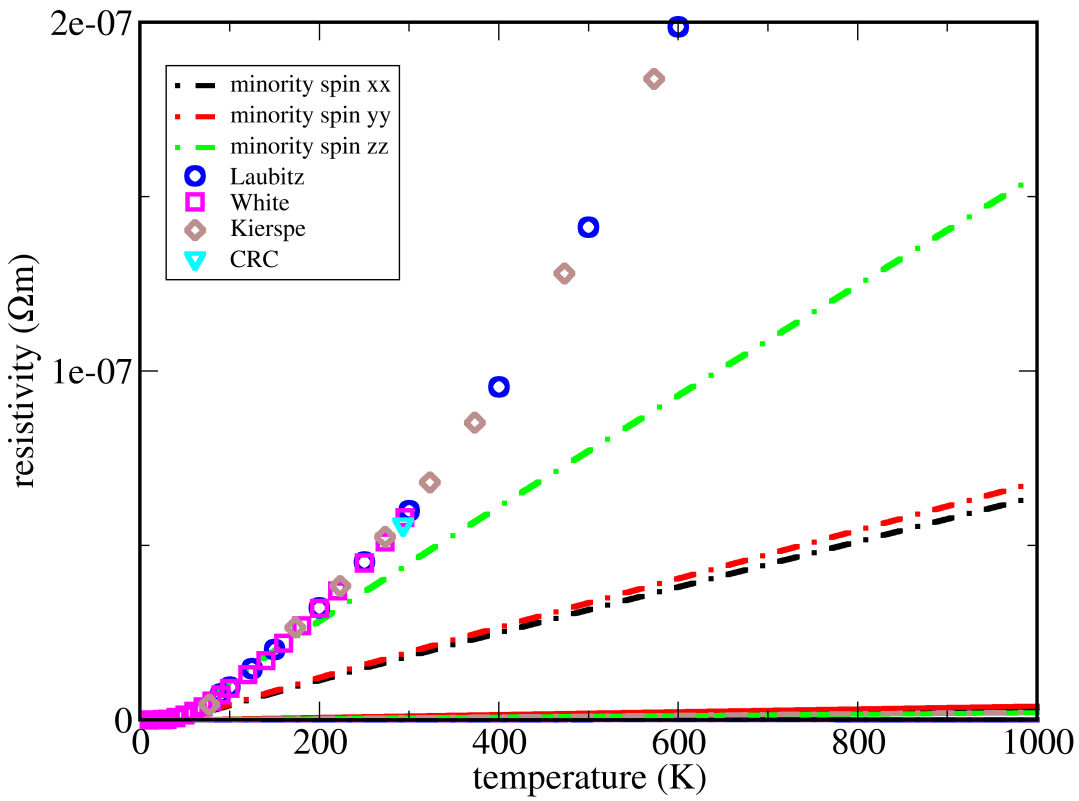

Figure 5. Electrical resistivity for spin polarized hcp Co, compared to experimental data from Refs [39, 40, 41, 42]. The low value of the EPC resistivity (which comes only from minority carriers) underestimates the experimental value after 200 K, mainly due to anharmonic effects. There is finally a phase transition to fcc Co at 660 K. The curves near 0 resistivity are majority spin diagonal terms and minority spin off diagonal terms in the conductivity matrix (see text).

a changing slope in the experimental data due to anharmonic effects. For Co $w(T)$ comes entirely from the phonon interactions with spin-down electrons. The overestimation of experiment is due to our neglect of impurity contributions, without which one would expect an average of the different directions for a polycrystalline sample. As noted above Co has a phase transition to fcc at 660 K, which will produce a further difference in $w(T)$ compared to our calculation.

5. Perspectives and conclusions

The possibility to separate the single spin contributions to experimental observables is quite challenging in practice. Certain materials with lower conduction electron densities, or with more complete polarization of states near E_F may be more amenable to direct comparison with calculations of the type presented here. We hope that this type of numerical analysis will stimulate more precise experiments. Measurements under

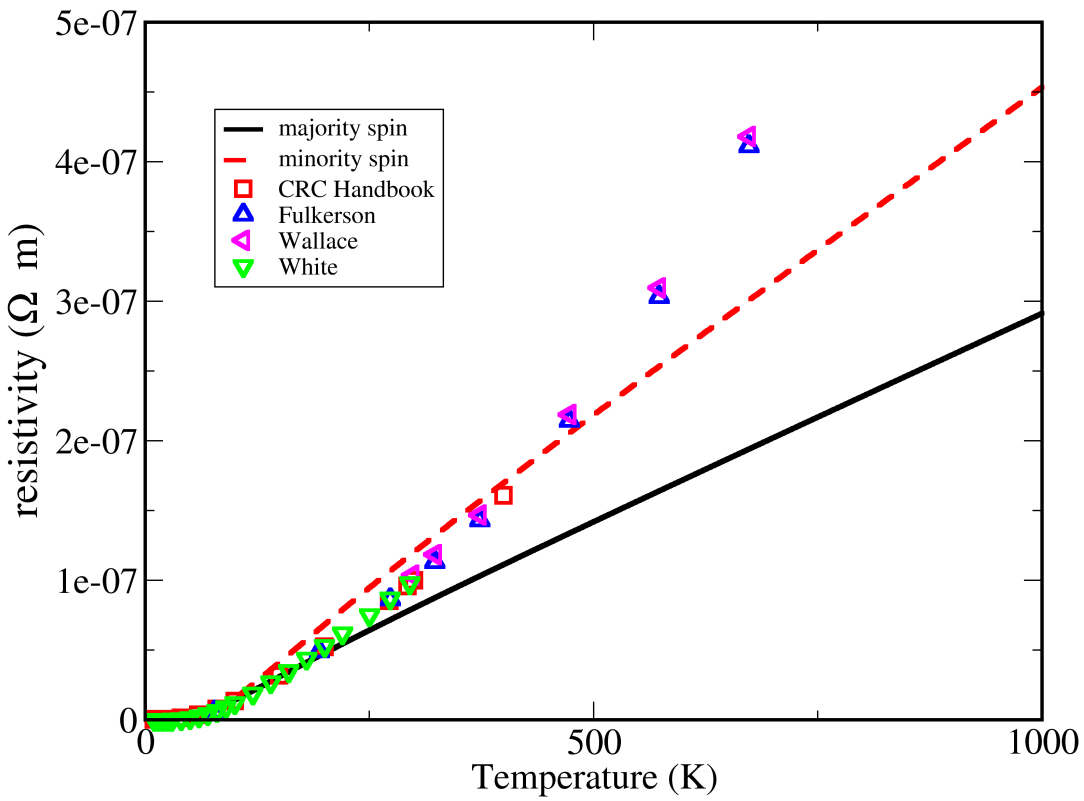

Figure 6. Electrical resistivity for spin polarized Fe, compared to experimental data from Refs [39, 43, 44, 41]. The experimental values fall between the extremal majority and minority spin values. The presence of spin flip centers (impurities or spin-orbit scattering) effectively averages the two resistances for the spin up and down channels.

applied field (taking care to separate Hall contributions to the current), in particular in a dynamical regime, could corroborate the very strong differences observed here in particular for Co. Phonon characterization with spin-polarized neutrons could also give explicit insight into spin-specific electron phonon coupling in ferromagnetic materials. Two important and related avenues for development are 1) the use of non-collinear spin formalisms and spin-orbit coupling, and 2) the inclusion of the interaction between phonons and magnons[49, 50]. Work is ongoing in both directions.

The spin-dependent electron-phonon coupling has been calculated ab initio in BCC iron and HCP cobalt, and compared to a range of available experimental data. The calculated phonon band structures are very accurate. Experimental electrical and thermal conductivities agree very well in Fe and are somewhat overestimated in Co, where the strong minority spin-phonon coupling is reduced by electron velocity effects. The inclusion of the correct magnetic state is crucial, both for the phonons and for the coupling, and opens the way for the first-principles determination of many new quantities in spintronics, high temperature magnetism, and complex magnetic systems.

Help with the OPIUM package from E. Walter and discussions with B. Xu are

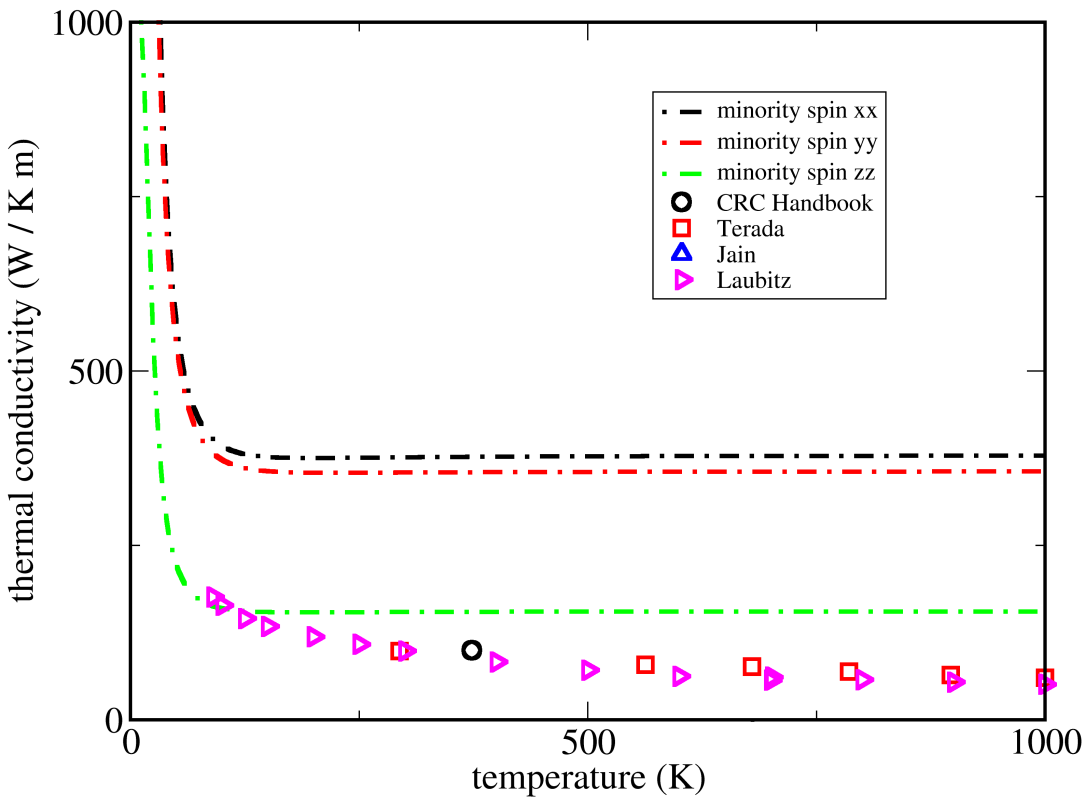

Figure 7. Thermal conductivity for spin polarized Co, compared to experimental data from Refs [39, 45, 46, 40]. The small EPC contribution translates to a strong overestimation of the thermal conductance: the main limitations to this calculation of w come from the neglect of impurities and phonon-phonon scattering, the latter becoming important at higher T. In Co the majority spin EPC is very weak (an order of magnitude smaller than minority) and the corresponding contribution to the conductivity is not shown.

gratefully acknowledged, as well as essential build system work on the ABINIT package by Y Pouillon. This research has been supported by the Belgian FNRS and the EU FP7 through the ETSF I3 e-I3 project (G.A. 211956). Computer time was provided by ULg-SEGI, UCL-CISM, the Red Española de Supercomputación (magerit machine), and by PRACE-2IP on Huygens and Hector (EU FP7 grant RI-283493). Funding from the Communauté française de Belgique (ARC 10/15-03 and a Crédit d'Impulsion) has been used in this work.

[1] Igor Žutić, Jaroslav Fabian, and S. Das Sarma. Spintronics: Fundamentals and applications. *Rev. Mod. Phys.*, 76:323–410, Apr 2004.

[2] Gerrit E.W. Bauer, Allan H. MacDonald, and Sadamichi Maekawa. Spin caloritronics? *Solid State Communications*, 150(11-12):459 – 460, 2010.

[3] Louis Taillefer. Scattering and pairing in cuprate superconductors. *Ann. Rev. Cond. Mat. Phys.*, 1:5170, 2010.

[4] O.K. Andersen and L. Boeri. On the multi-orbital band structure and itinerant magnetism of iron-based superconductors. *Ann. der Physik*, 523(1-2):8–50, 2011.

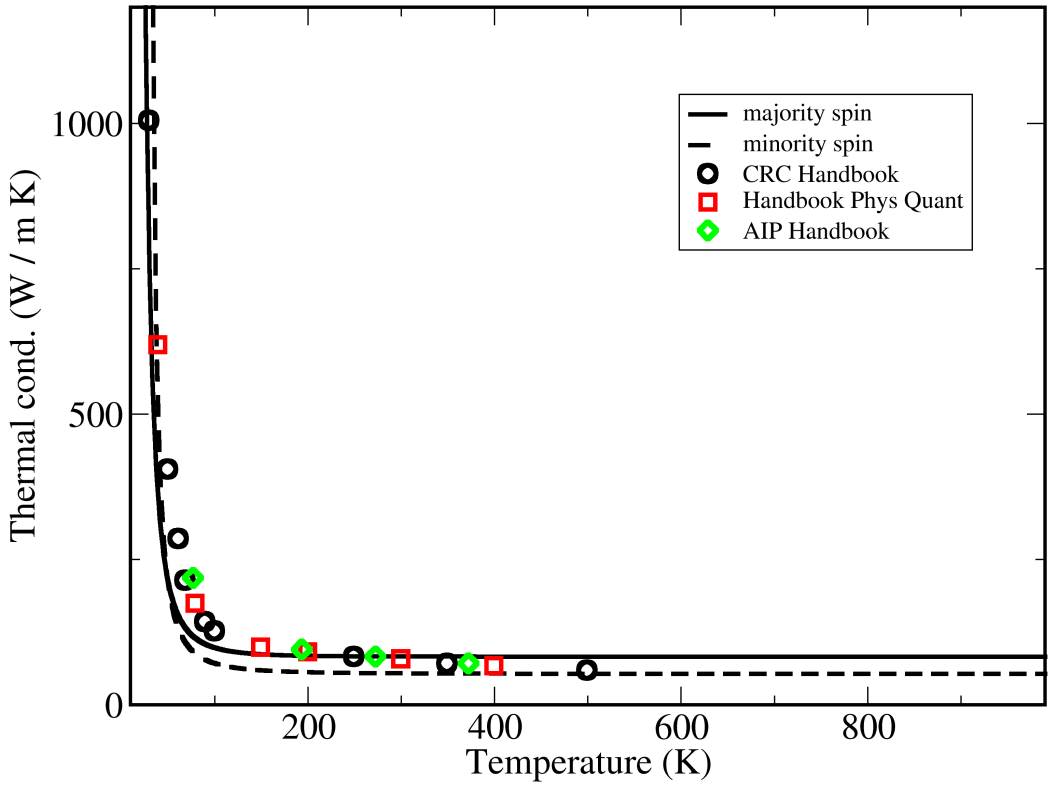

Figure 8. Thermal conductivities for spin polarized Fe, compared to experimental data from Refs [39], [47] and [48]. The agreement is comparable to that of Ref [12].

[5] Monica Pozzo, Chris Davies, David Gubbins, and Dario Alfe. Thermal and electrical conductivity of iron at earth/'s core conditions. *Nature*, page 1476, 2012.

[6] P. Hohenberg and W. Kohn. Inhomogeneous electron gas. *Phys. Rev.*, 136:864–871, 1964.

[7] W. Kohn and L. J. Sham. Self-consistent equations including exchange and correlation effects. *Phys. Rev.*, 140:A 1133 – A 1138, 1965.

[8] Stefano Baroni, Stefano de Gironcoli, Andrea Dal Corso, and Paolo Giannozzi. Phonons and related crystal properties from density-functional perturbation theory. *Rev. Mod. Phys.*, 73:515, 2001.

[9] X. Gonze. First-principles responses of solids to atomic displacements and homogeneous electric fields: Implementation of a conjugate-gradient algorithm. *Phys. Rev. B*, 55:10337, 1997.

[10] X. Gonze and C. Lee. Dynamical matrices, born effective charges, dielectric permittivity tensors, and interatomic force constants from density-functional perturbation theory. *Phys. Rev. B*, 55:10355, 1997.

[11] L. Boeri, M. Calandra, I. I. Mazin, O. V. Dolgov, and F. Mauri. Effects of magnetism and doping on the electron-phonon coupling in $bafe_2as_2$. *Phys. Rev. B*, 82:020506, Jul 2010.

[12] Xianwei Sha and R E Cohen. First-principles studies of electrical resistivity of iron under pressure. *J. Phys.: Cond. Matt.*, 23(7):075401, 2011.

[13] Sven Essert and Hans Christian Schneider. Electron-phonon scattering dynamics in ferromagnetic metals and their influence on ultrafast demagnetization processes. *Phys. Rev. B*, 84:224405, Dec 2011.

[14] T Jarlborg. Spin fluctuations, electron-phonon coupling and superconductivity in near-magnetic

elementary metals: Fe, co, ni and pd. *Physica C: Supercond.*, 385(4):513 – 524, 2003.

[15] F. Körmann, A. Dick, B. Grabowski, B. Hallstedt, T. Hickel, and J. Neugebauer. Free energy of bcc iron: Integrated ab initio derivation of vibrational, electronic, and magnetic contributions. *Phys Rev B*, 78:033102, 2008.

[16] Henry Ehrenreich, Frederick Seitz, and David Turnbull, editors. *Theory of Superconducting T_c*, volume 37 of *Solid State Phys.* Academic Press, New York, 1982.

[17] P. B. Allen. Fermi-surface harmonics: A general method for nonspherical problems. application to boltzmann and eliashberg equations. *Phys. Rev. B*, 13:1416–1427, 1976.

[18] S. Y. Savrasov and D. Y. Savrasov. Electron-phonon interactions and related physical properties of metals from linear-response theory. *Phys. Rev. B*, 54:16487, 1996.

[19] S Savrasov. Linear response calculations of spin fluctuations. *Phys. Rev. Lett.*, 81:2570, 1998.

[20] Paweł Buczek, Arthur Ernst, and Leonid M. Sandratskii. Different dimensionality trends in the landau damping of magnons in iron, cobalt, and nickel: Time-dependent density functional study. *Phys. Rev. B*, 84:174418, 2011.

[21] X. Gonze, G.-M. Rignanese, M. Verstraete, J.-M. Beuken, Y. Pouillon, R. Caracas, F. Jollet, M. Torrent, G. Zerah, M. Mikami, Ph. Ghosez, M. Veithen, V. Olevano, L. Reining, R. Godby, G. Onida, D. Hamann, and D. C. Allan. A brief introduction to the abinit software project. *Zeit. für Kristall.*, 220:558–562, 2005.

[22] E.J. Walter and A Rappe. Opium pseudopotential package. http://opium.sourceforge.net/.

[23] A.M. Rappe, K.M. Rabe, E. Kaxiras, and J.D. Joannopoulos. Optimized pseudopotentials. *Phys. Rev. B*, 41(2):1227–1230, 1990.

[24] Steven G. Louie, S. Froyen, and M. L. Cohen. Nonlinear ionic pseudopotentials in spin-density-functional calculations. *Phys. Rev. B*, 26:1738, 1982.

[25] John P. Perdew, K Burke, and M Ernzerhof. Generalized gradient approximation made simple. *Phys. Rev. Lett.*, 77:3865, 1996.

[26] V.I. Anisimov, J. Zaanen, and O.K. Andersen. Band theory and mott insulators: Hubbard u instead of stoner i. *Phys. Rev. B*, 44:943, 1991.

[27] N. Wakabayashi, R. H. Scherm, and H. G. Smith. Lattice dynamic of ti, co, tc, and other hcp transition metals. *Phys. Rev. B*, 25:5122–5132, Apr 1982.

[28] F. Vincent and M. Figlarz. Quelques précisions sur les paramètres cristallins et l'intensité des raies debye-scherrer du cobalt cubique et du cobalt hexagonal. *C. R. Hebd Séances Acad Sci.*, 264C:1270, 1967.

[29] Víctor Antonio de la Peña O'Shea, Iberio de P. R. Moreira, Alberto Roldán, and Francesc Illas. Electronic and magnetic structure of bulk cobalt: The alpha, beta, and epsilon-phases from density functional theory calculations. *J. Chem. Phys.*, 133(2):024701, 2010.

[30] G. J. McMullan, D. D. Pilgram, and A. Marshall. Fermi surface and band structure of ferromagnetic cobalt. *Phys. Rev. B*, 46:3789–3797, Aug 1992.

[31] Mathias Ekman, Babak Sadigh, Kristin Einarsdotter, and Peter Blaha. Ab initio study of the martensitic bcc-hcp transformation in iron. *Phys. Rev. B*, 58:5296–5304, Sep 1998.

[32] J. F. van Acker, Z. M. Stadnik, J. C. Fuggle, H. J. W. M. Hoekstra, K. H. J. Buschow, and G. Stroink. Magnetic moments and x-ray photoelectron spectroscopy splittings in fe *3s* core levels of materials containing fe. *Phys. Rev. B*, 37:6827–6834, Apr 1988.

[33] Marco Cazzaniga, Lucia Caramella, Nicola Manini, and Giovanni Onida. *Ab initio* intraband contributions to the optical properties of metals. *Phys. Rev. B*, 82:035104, Jul 2010.

[34] M. Dixon, F. E. Hoare, T. M. Holden, and D. E. Moody. The low temperature specific heats of some pure metals (cu, ag, pt, al, ni fe co). *Proc. R. Soc. London, Ser. A*, 285:561–580, 1965.

[35] B.N. Brockhouse, H.E. Abou-Helal, and E.D. Hallman. Lattice vibrations in iron at 296k. *Solid State Comm.*, 5(4):211 – 216, 1967.

[36] Andrea Dal Corso and Stefano de Gironcoli. *Ab initio* phonon dispersions of fe and ni. *Phys. Rev. B*, 62:273–277, Jul 2000.

[37] P. Modak, A. K. Verma, R. S. Rao, B. K. Godwal, and R. Jeanloz. *Ab initio* total-energy and

phonon calculations of co at high pressures. *Phys. Rev. B*, 74:012103, Jul 2006.

[38] Jack Bass and William P Pratt Jr. Spin-diffusion lengths in metals and alloys, and spin-flipping at metal/metal interfaces: an experimentalist's critical review. *J. Phys. Cond. Matt.*, 19:183201, 2007.

[39] David R. Lide, editor. *CRC Handbook of Chemistry and Physics*. CRC Press, Cleveland, OH, 87 edition, 2006.

[40] M.J. Laubitz and T. Matsumura. Transport properties of the ferromagnetic metals. i. cobalt. *Can. J. Phys.*, 51:1247, 1973.

[41] G.K. White and S.B. Woods. Electrical and thermal resistivity of the transition elements at low temperatures. *Phil. Trans. Roy. Soc.*, A251:273, 1959.

[42] W. Kierspe, R. Kohlhaas, and H. Gonska. *Z. Angew. Phys.*, 24:28, 1967.

[43] W. Fulkerson, J.P. Moore, and D.L. McElroy. Comparison of the thermal conductivity, electrical resistivity, and seebeck coefficient of a high purity iron and an armco iron to 1000° c. *J. Appl. Phys.*, 37:2639, 1966.

[44] D.C. Wallace, P.H. Sidles, and G.C. Danielson. Specific heat of high purity iron by a pulse heating method. *J. Appl. Phys.*, 31:168, 1960.

[45] S. C. Jain, V. Narayan, and T. C. Goel. Thermal conductivity of metals at high temperatures by the jain and krishnan method ii. cobalt. *J. Phys. D: Appl. Phys.*, 2:101, 1969.

[46] Yoshihiro Terada, Kenji Ohkubo, Tetsuo Mohri, and Tomoo Suzuki. Thermal conductivity of cobalt-base alloys. *Metal. Mat. Trans. A*, 34A:2–26, 2003.

[47] I.S. Grigoriev and E.Z. Meilikhov, editors. *Handbook of Physical quantities*. CRC Press, Boca Raton, FL, 1997.

[48] D.E. Gray, editor. *American Institute of Physics Handbook*. McGraw-Hill, New York, 3 edition, 1972.

[49] S. Petit, F. Moussa, M. Hennion, S. Pailhès, L. Pinsard-Gaudart, and A. Ivanov. Spin phonon coupling in hexagonal multiferroic ymno3. *Phys. Rev. Lett.*, 99:266604, 2007.

[50] M. Braden, B. Hennion, W. Reichardt, G. Dhalenne, and A. Revcolevschi. Spin-phonon coupling in cugeo3. *Phys. Rev. Lett.*, 80:3634, 1998.